



HAL
open science

Dietary strategies of Pleistocene Pongo sp. and Homo erectus on Java (Indonesia)

Jülide Kubat, Alessia Nava, Luca Bondioli, M Christopher Dean, Clément Zanolli, Nicolas Bourgon, Anne-Marie Bacon, Fabrice Demeter, Beatrice Peripoli, Richard Albert, et al.

► **To cite this version:**

Jülide Kubat, Alessia Nava, Luca Bondioli, M Christopher Dean, Clément Zanolli, et al.. Dietary strategies of Pleistocene Pongo sp. and Homo erectus on Java (Indonesia). *Nature Ecology & Evolution*, 2023, 7, pp.279-289. 10.1038/s41559-022-01947-0 . hal-03987629

HAL Id: hal-03987629

<https://hal.science/hal-03987629>

Submitted on 16 Oct 2023

HAL is a multi-disciplinary open access archive for the deposit and dissemination of scientific research documents, whether they are published or not. The documents may come from teaching and research institutions in France or abroad, or from public or private research centers.

L'archive ouverte pluridisciplinaire **HAL**, est destinée au dépôt et à la diffusion de documents scientifiques de niveau recherche, publiés ou non, émanant des établissements d'enseignement et de recherche français ou étrangers, des laboratoires publics ou privés.

Dietary strategies of Pleistocene *Pongo* sp. and *Homo erectus* on Java (Indonesia)

Jülide Kubat 1,2,3 , Alessia Nava 4 , Luca Bondioli 5,6, M. Christopher Dean 7, Clément Zanolli 8, Nicolas Bourgon 9, Anne-Marie Bacon 3, Fabrice Demeter 10,11, Beatrice Peripoli 6, Richard Albert 1,12, Tina Lüdecke 13,14, Christine Hertler 2,15, Patrick Mahoney 4, Ottmar Kullmer 2,16, Friedemann Schrenk 2,16 & Wolfgang Müller 1,12,17

1Frankfurt Isotope and Element Research Center (FIERCE), Goethe University Frankfurt, Frankfurt, Germany. 2Department of Palaeoanthropology, Senckenberg Research Institute and Natural History Museum Frankfurt, Frankfurt, Germany. 3Université Paris Cité, CNRS, BABEL, Paris, France. 4Skeletal Biology Research Centre, School of Anthropology and Conservation, University of Kent, Canterbury, UK. 5Bioarchaeology Service, Museum of Civilizations, Rome, Italy. 6Department of Cultural Heritage, University of Padova, Padova, Italy. 7Department of Earth Sciences, Natural History Museum, London, UK. 8University of Bordeaux, CNRS, MCC, PACEA, UMR 5199, Pessac, France. 9Department of Human Evolution, Max Planck Institute for Evolutionary Anthropology, Leipzig, Germany. 10Lundbeck Foundation GeoGenetics Centre, GLOBE Institute, University of Copenhagen, Copenhagen, Denmark. 11Eco-anthropologie (EA), Muséum National d'Histoire Naturelle, CNRS, Université de Paris, Paris, France. 12Institute of Geosciences, Goethe University Frankfurt, Frankfurt, Germany. 13Emmy Noether Group for Hominin Meat Consumption, Max Planck Institute for Chemistry, Mainz, Germany. 14Senckenberg Biodiversity and Climate Research Centre, Frankfurt, Germany. 15ROCEEH Research Centre, Heidelberg Academy of Sciences and Humanities, Heidelberg, Germany. 16Department of Paleobiology and Environment, Institute of Ecology, Evolution, and Diversity, Goethe University Frankfurt, Frankfurt, Germany. 17Senckenberg Research Institute and Natural History Museum Frankfurt, Frankfurt, Germany.

e-mail: julide.kubat@gmail.com; alessianava@gmail.com; w.muller@em.uni-frankfurt.de

During the Early to Middle Pleistocene, Java was inhabited by hominid taxa of great diversity. However, their seasonal dietary strategies have never been explored. We undertook geochemical analyses of orangutan (*Pongo* sp.), *Homo erectus* and other mammalian Pleistocene teeth from Sangiran. We reconstructed past dietary strategies at subweekly resolution and inferred seasonal ecological patterns. Histologically controlled spatially resolved elemental analyses by laser-based plasma mass spectrometry confirmed the preservation of authentic biogenic signals despite the effect of spatially restricted diagenetic overprint. The Sr/Ca record of faunal remains is in line with expected trophic positions, contextualizing fossil hominid diet. *Pongo* sp. displays marked seasonal cycles with ~3 month-long strongly elevated Sr/Ca peaks, reflecting contrasting plant food consumption presumably during the monsoon season, while lower Sr/Ca ratios suggest different food availability during the dry season. In contrast, omnivorous *H. erectus* shows low and less accentuated intra-annual Sr/Ca variability compared to *Pongo* sp., with $\delta^{13}\text{C}$ data of one individual indicating a dietary shift from C4 to a mix of C3 and C4 plants. Our data suggest that *H. erectus* on Java was maximizing the resources available in more open mosaic habitats and was less dependent on variations in seasonal resource availability. While still influenced by seasonal food availability, we infer that *H. erectus* was affected to a lesser degree than *Pongo* sp., which inhabited monsoonal rain forests on Java. We suggest that *H. erectus* maintained a greater degree

of nutritional independence by exploiting the regional diversity of food resources across the seasons.

The Pleistocene hominid fossil record from the Sangiran Dome in Central Java, Indonesia, is one of the largest palaeoanthropological collections in Southeast Asia, evidencing an Early Pleistocene expansion of *Homo erectus* onto the Sunda Shelf^{1–4}. The high morphodimensional variability of Indonesian hominid specimens led in the past to the attribution of the fossils to a variety of taxa such as *H. erectus*, *Meganthropus palaeojavanicus*, *Pithecanthropus dubius* or *Pongo* sp. and has fuelled taxonomic debates^{1,5–9}. Recently, a high level of Javanese hominid palaeodiversity was revealed, which confirmed the taxonomic validity of the genus *Meganthropus*, a taxon that coexisted with *H. erectus* and *Pongo*¹⁰. Although dental macrowear and enamel thickness broadly reflect different dietary adaptations among these hominids¹⁰, little is known spectrometry to retrieve time-resolved information from their dental enamel about dietary diversity throughout the lives of individual early hominins, in conjunction with stable isotope analysis. For decades, geochemical analyses—primarily $\delta^{13}\text{C}$ and $\delta^{18}\text{O}$ measurements—of tooth enamel have been used to retrieve palaeoenvironment, palaeodiet and life history information of extinct hominins such as *Australopithecus*^{11–13}, *Paranthropus*^{11,13–15} and Neanderthals^{16,17}. This method has seen only limited application to hominins in Southeast Asia, with the exception of our own species. Consequently, we explored for the first time strontium/calcium (Sr/Ca) and barium/calcium (Ba/Ca) ratios and other trace elemental signals at high spatial/time resolution in the dental enamel of premolars and molars, to assess dietary and life history signals in Pleistocene *H. erectus* and *Pongo* sp. from the Sangiran Dome. Tooth enamel—contrary to bone and dentine—is less prone to postmortem diagenetic alteration due to its highly mineralized nature^{18,19}. Moreover, it is secreted and mineralized sequentially in utero and during infancy to early adolescence and, once fully mineralized, remains compositionally and structurally stable during life. Consequently, enamel captures and preserves environmental and dietary changes that occur during the enamel development phases in an individual’s life^{20–23}. The incremental nature of tooth growth allows us to resolve shifts in enamel composition that relate directly to life history at near-(sub)weekly resolution. Moreover, tooth tissues in themselves contain information of potential taxonomic value²¹. The longer period rhythms in dental enamel (striae of Retzius periodicity, RP) have been used to infer taxonomic affinity in certain Far Eastern fossil specimens²⁴. Indeed, elemental and isotopic analysis by laser-ablation inductively-coupled-plasma mass spectrometry (LA-ICPMS) across the incremental structures of sequentially secreted enamel provides a temporally and spatially highly resolved record of an individual’s childhood. Such data allow the interpretation of diet, health, growth rates, weaning and mobility as well as changes of the environmental setting on a seasonal to weekly scale^{16,17,25–27}. Trace element ratios Sr/ Ca and Ba/Ca in dental enamel can record dietary signals due to the biopurification of Ca in trophic chains^{28–30}. The higher the trophic level, the less [Sr] and [Ba] relative to [Ca] are incorporated into enamel, resulting in higher values of trace element ratios in herbivore enamel than in omnivores or carnivores^{11,28,31}, although additional factors such as soil ingestion play a role³². For comparison and as a trophic level reference for the Sangiran hominids, we used isolated premolars and molars of mammalian specimens belonging to different families (Felidae, Rhinocerotidae, Suidae, Cervidae and Hippopotamidae; Table 1) from the Sangiran fossil assemblage presumably co-existing with various hominid taxa such as *H. erectus*, *Meganthropus* and *Pongo*^{10,33,34}. All specimens were recovered from either the Early Pleistocene Sangiran Formation or from the later Early to initial Middle Pleistocene Bapang Formation, as both are fossiliferous and contain distinct faunal assemblages and

taxa^{4,35,36}. However, the exact stratigraphic allocation of all specimens is not documented^{2,36}. The geological ages of the specimens range between 1.4 to 1.0 million years ago (Ma) and 1.0 to 0.7 Ma for specimens from the Sangiran and Bapang Formations, respectively⁴. We focused our study on Sr/Ca (and to a lesser extent Ba/Ca) ratios as (relative) trophic level proxies, including an assessment of how well biogenic geochemical information is preserved in Pleistocene bioapatite from (sub)tropical contexts by using elements Mn, Al, Y, Ce, U as tracers of postmortem alteration^{17,31,32,37–41}. Previous stable isotope analyses of *H. erectus* bone samples from Sangiran were not successful in obtaining palaeoecological signals due to diagenetic alteration of bone tissue⁴². Here, we include sequentially microsampled carbon ($\delta^{13}\text{C}$) and oxygen ($\delta^{18}\text{O}$) isotope analyses of dental enamel of one *H. erectus* permanent premolar (S7-37) to contextualize our elemental results and obtain additional dietary/environmental information.

Table 1 | List of specimens from the Gustav Heinrich Ralph von Koenigswald collection used in the present study.

	Catalogue number	Taxonomic identification	Dental elements
Primates	S7-13	Hominidae/ <i>H. erectus</i>	Upper left M
	S7-37	Hominidae/ <i>H. erectus</i>	Right P ⁴
	SMF-8865	Hominidae/ <i>H. erectus</i>	Lower left M
	SMF-8864	Hominidae/ <i>Pongo</i> sp.	Lower right M
Carnivora	SMF/PA/F6664	Felidae/ <i>Panthera tigris</i>	Right P ₄
	SMF/PA/F6666	Felidae/ <i>P. tigris</i>	Right M ₁
Perissodactyla	SMF/PA/F5941	Rhinocerotidae/ <i>Rhinoceros sondaicus</i>	Left M ₁
	SMF/PA/F5950	Rhinocerotidae/ <i>R. sondaicus</i>	Left M ₂
Artiodactyla	SMF/PA/F738	Suidae/ <i>Sus</i> sp.	Right M ³
	SMF/PA/F869	Suidae/ <i>Sus</i> sp.	Right M ³
	SMF/PA/F5077	Cervidae/ <i>Axis lydekkeri</i>	Left M ₂
	SMF/PA/F5258	Cervidae/ <i>A. lydekkeri</i>	Right P ³ , M ¹ , M ² , M ³
	SMF/PA/F6	Hippopotamidae/ <i>Hexaprotodon</i> sp.	Right M ²
	SMF/PA/F53	Hippopotamidae/ <i>Hexaprotodon</i> sp.	Left M ₂

The specimens are housed in the Department of Palaeoanthropology, Senckenberg Research Institute and Natural History Museum Frankfurt, Frankfurt, Germany. M, molar; P, premolar.

Results

In Supplementary Table 2 we report Retzius periodicity (RP), laser track length and the corresponding time span for the analysed samples. The RP of *Pongo* sp. SMF-8864 was obtained through direct counts of cross-striations between two adjacent Retzius lines. The RP of *H. erectus* SMF-8865, given the section thickness necessary for chemical analyses and the presence of some accentuated markings, was calculated as the distance between adjacent Retzius lines divided by local daily secretion rate (DSR); the latter directly measured in areas of the section where the cross-striations were clearly visible. For *H. erectus* S7-37 P4, we report the RP calculated in ref. 21 for the S7-37 M1 belonging to the same individual. Elemental signals were retrieved within enamel close ($<100\ \mu\text{m}$) to the enamel-dentine-junction (EDJ) because it is where environmental signals are best captured topographically during secretion and elemental overprint during enamel maturation has the least effect^{17,26,43–45}. For assessing postmortem diagenetic overprint, scatter plots of [Sr] or [Ba] versus [Mn] or [U] at EDJ profiles of representative samples of each trophic level were generated (Fig. 1 and Extended Data Fig. 1). All cases show clearly positive correlations between trace elements and diagenesis-indicating element concentrations. Even though multistage diagenetic histories may be indicated by different trajectories (Fig. 1), uptake of Sr and Ba with increasing geochemical alteration is evident, which implies that the best approximations of initial biogenic [Sr] or [Ba] (or expressed as Sr/Ca, Ba/Ca ratios) can be found at lowest [Mn] or [U]. These plots also reveal that [Sr] increases by a maximum of $\sim 180\%$, while [Ba] is characterized by a threefold to tenfold increase, confirming the higher susceptibility of Ba to postmortem overprint. Repeat profiles at the EDJs of both tooth aspects and along prism directions indicate greater consistency between corresponding Sr/Ca profiles, relative to those of Ba/Ca (Extended Data Figs. 2–6). Using [Mn] and [U] thresholds of 400 and 1 ppm, respectively, to screen Sr/Ca and Ba/Ca trophic level signals, revealed expected patterns for trophic groups for Fig. 7). As a result, we focus more on Sr/Ca results but also note that Ba/Ca can indicate reliable results in case of well-preserved samples (for example, *Pongo* SMF-8864, see below). The Sr/Ca ratio boxplots of faunal and hominid specimens (Fig. 2) show carnivorous Felidae with the lowest Sr/Ca ratio in the faunal assemblage ($\sim 8.4 \times 10^{-4}$), following the expected trophic level trend towards lower Sr/Ca ratios relative to omnivores ($\sim 1.1 \times 10^{-3}$; represented by Suidae) and different herbivore groups (1.6×10^{-3} to 4.0×10^{-3}). Rhinocerotidae exhibit a Sr/Ca level about two times higher than all other herbivores and a broad Sr/Ca variability. The three *H. erectus* dental specimens yield Sr/Ca ratios between those of the Felidae and Suidae. The *Pongo* sp. specimen SMF-8864 shows the largest variation in Sr/Ca distribution among all taxa and has many distributional outliers towards higher Sr/Ca values (Fig. 2). Its median value fits well within the Hippopotamidae and Cervidae central distributions. The peculiar distribution of Sr/Ca values in *Pongo* sp. SMF-8864 is the result of distinct biogenic Sr/Ca peaks throughout the life of this individual and not of diagenetic origin, as shown by the diagenetic indicators (see below). The elemental ratio profiles in hominid tooth enamel were aligned with the individual odontochronologies (Figs. 3 and 4 and Extended Data Figs. 2–6) on both lingual and buccal aspects (except for S7-37 P4 where only the buccal aspect was available for analysis) to derive Sr/Ca (and Ba/Ca) variation versus time (secretion–days). Only for S7-37 P4 the life time referred to birth is available following ref. 46 but not for molars with uncertain positions such as S7-13, SMF-8864 and SMF-8865, although we tentatively attribute molar positions on the basis of some diagnostic morphological features described in the Supplementary Information and corresponding chemical signals. Figure 3a shows the Sr/Ca and Ba/Ca EDJ profiles together with diagenesis-indicating [U] and [Mn] against time for the 1,073 d (~ 2 yr and 11 months) of the buccal aspect of the *Pongo* sp. SMF-8864 molar. EDJ (Fig. 3a) and corresponding prisms (Fig.

3b and Extended Data Fig. 4) Sr/Ca profiles for the buccal enamel show good agreement but along the prisms invariably lower Sr/Ca values towards outer enamel (Fig. 3b), as expected by the effect of maturation overprint²⁶.

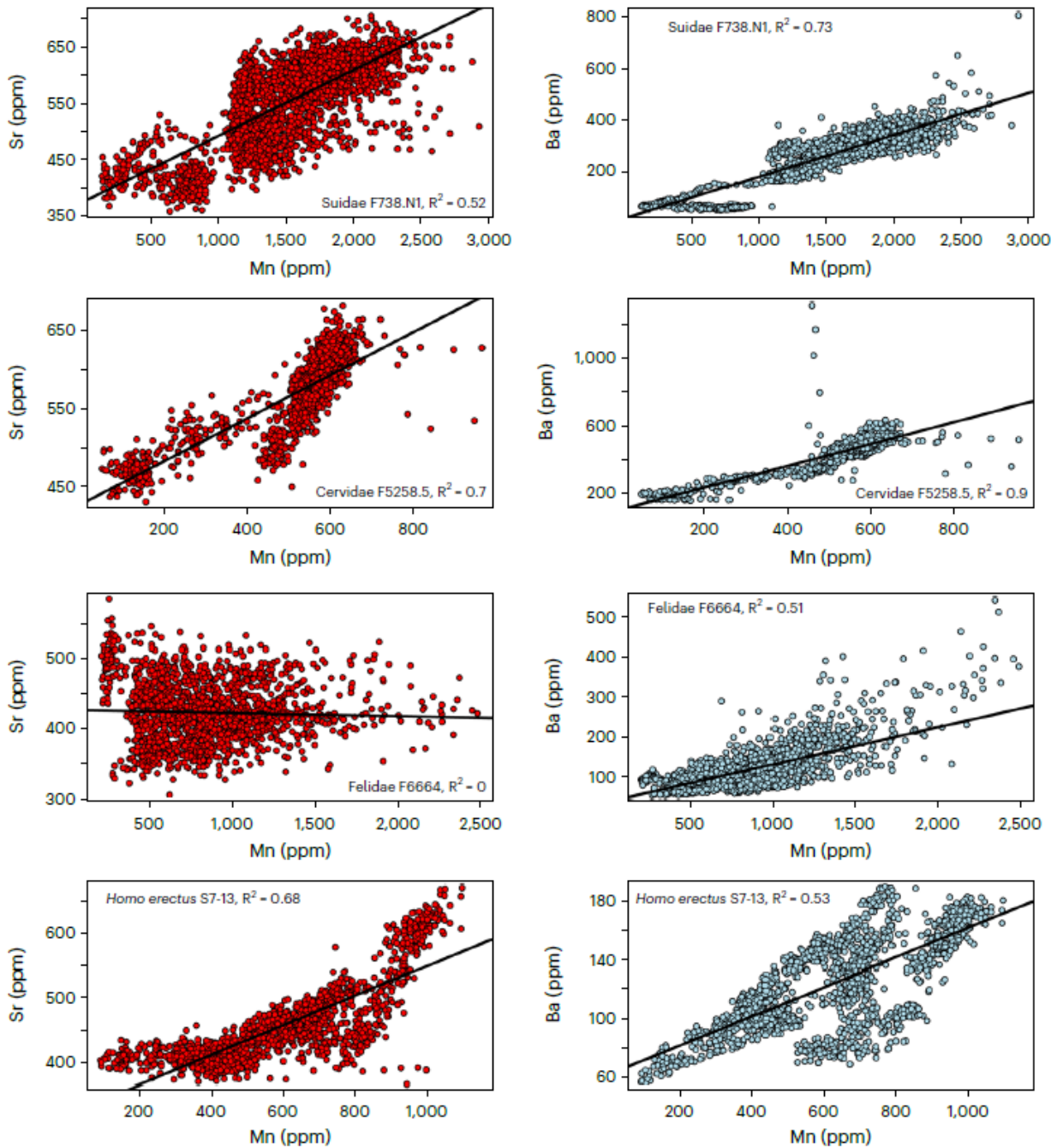


Fig. 1 | Scatter plots of [Sr] or [Ba] versus [Mn], respectively, for representative examples of each faunal group. Respective plots illustrate the diagenesis assessment of the fossil assemblage. See Extended Data Fig. 1 for equivalent plots relative to [U]. For simplicity, data are here shown as concentrations, whereas elsewhere they are displayed as Element/Ca to facilitate comparison.

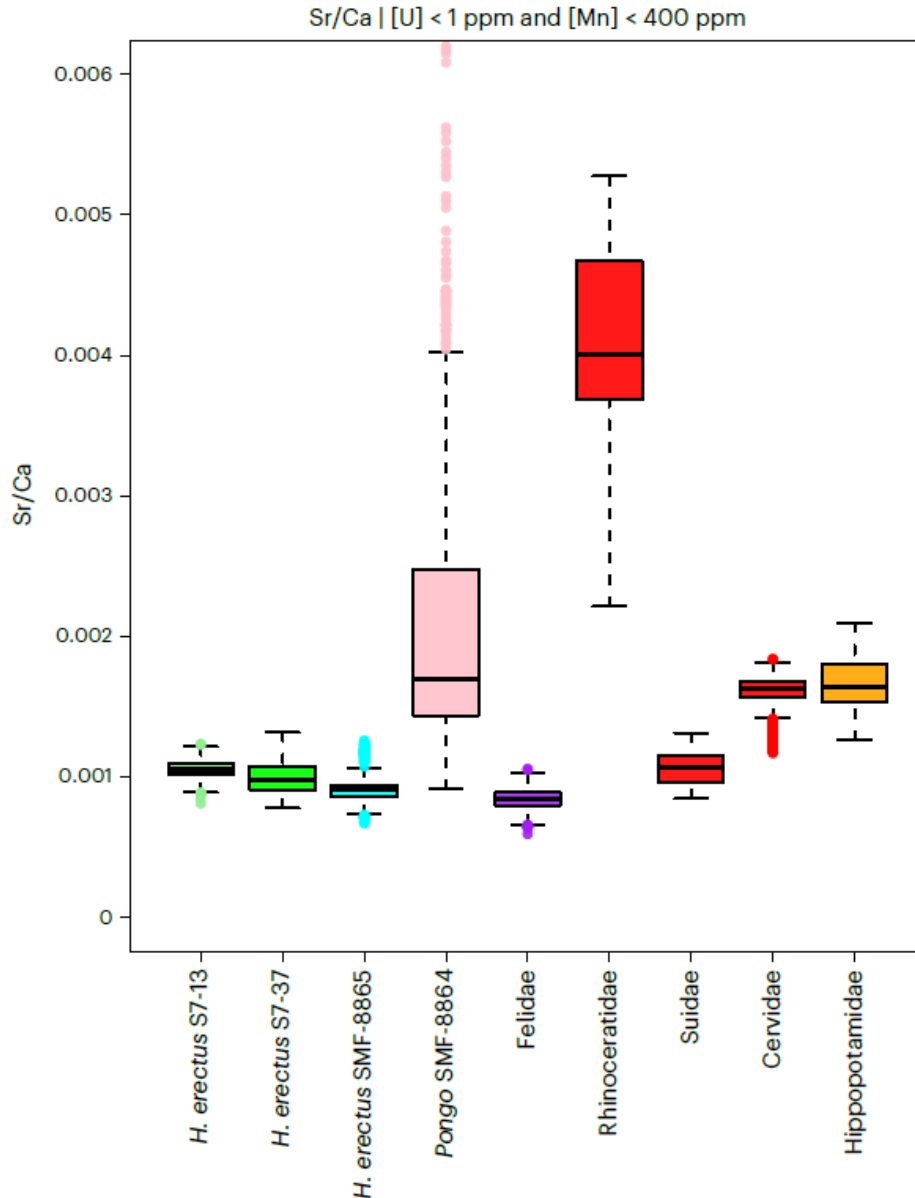


Fig. 2 | Sr/Ca ratios boxplots of faunal and hominid specimens. Boxplots comparing *H. erectus* and *Pongo* sp. specimens to other taxa with known trophic levels, all displayed after diagenesis filtering, that is [U] < 1 ppm and [Mn] < 400 ppm ($\mu\text{g g}^{-1}$) (Extended Data Fig. 7). Coloured dots outside the whiskers represent outliers, lower whisker is equal to minimum value (excluding outliers), lower hinge equals to first quartile, thick line represents the median value, upper hinge equals to third quartile and upper whisker to maximum value (excluding outliers). The numerous outliers in *Pongo* sp. SMF-8864 correspond to biogenic peaks explained in Fig. 3. *H. erectus* S7-13 number of points = 1,032; *H. erectus* S7-37 points = 1,012; *H. erectus* SMF-8865 points = 606; *Pongo* SMF-8864 points = 708; Felidae points = 3,232, number of samples = 2; Rhinocerotidae points = 631, samples = 2; Suidae points = 189, samples = 2; Cervidae points = 920, samples = 2; and Hippopotamidae points = 1,263, samples = 2.

The buccal and lingual Sr/Ca EDJ profiles of *Pongo* sp. SMF-8864 are compared in Fig. 3c to assess the reproducibility of in vivo elemental signals. The time span covered by the lingual aspect is 1,339 d (~3 yr and 8 months; Fig. 3c).

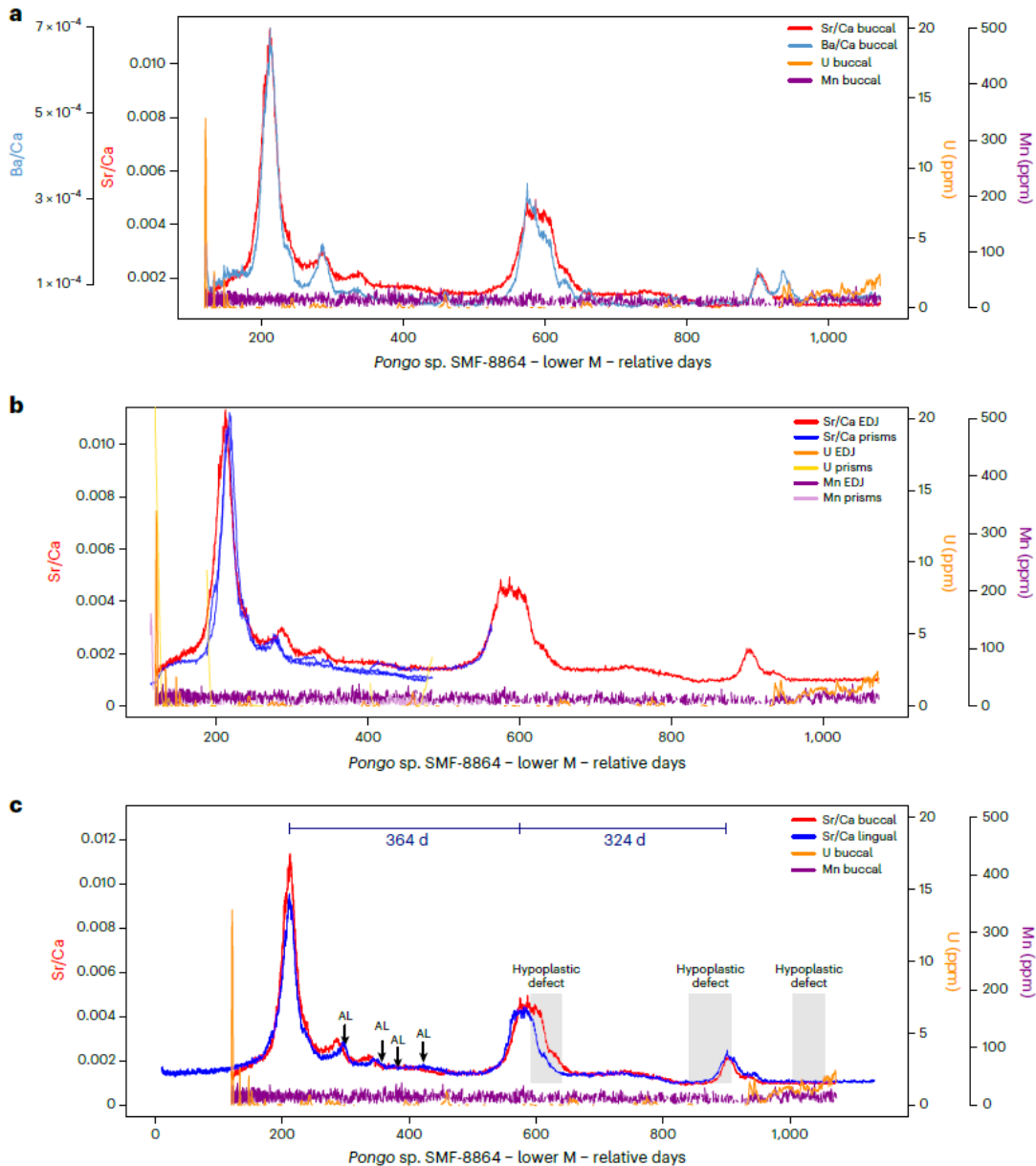


Fig. 3 | Time-resolved compositional profiles for *Pongo* sp. SMF-8864 molar. a, Sr/Ca, Ba/Ca, [U] and [Mn] along the EDJ plotted against relative days. Apart from isolated [U] peaks, only minor diagenetic overprint is discernible for thin enamel from ~925 d. b, Comparative Sr/Ca, [U] and [Mn] profiles along EDJ versus corresponding prism orientations (Extended Data Fig. 4), plotted against relative days; while data agree well overall, towards outer enamel the latter show lower Sr/Ca values relative to corresponding EDJ positions due to maturation overprint. c, Elemental profiles for both mesiolingual and mesio Buccal cusp showcase the remarkable similarity of Sr/Ca on both enamel sides. AL and hypoplastic defects are highlighted. See text for details.

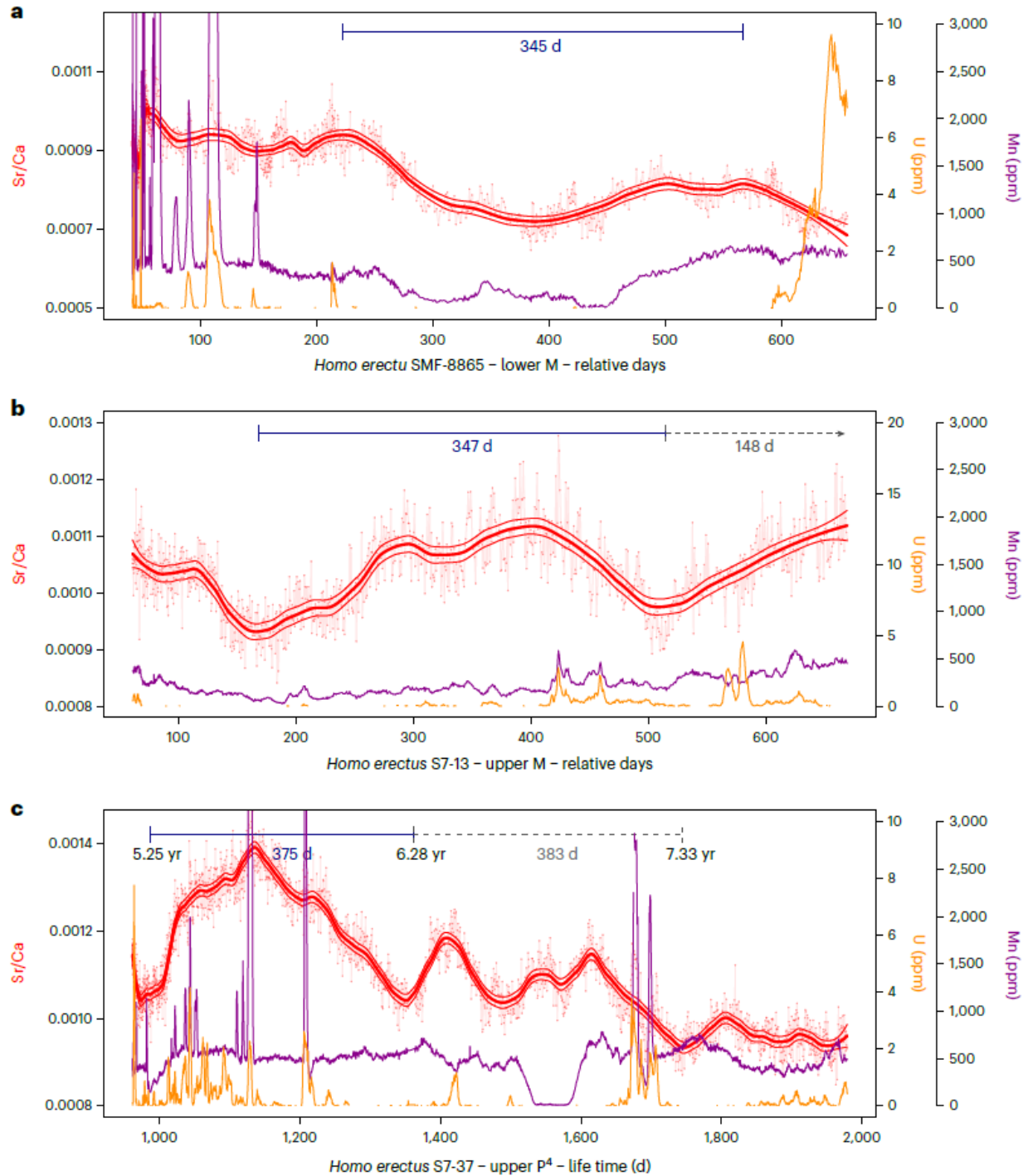


Fig. 4 | Time-resolved compositional EDJ profiles for all investigated *H. erectus* specimens. EDJ profiles of *H. erectus* specimens plotted against their individual relative dental chronologies except for S7-37 P4 where odontochronology in life time is known. a, SMF-8865. b, S7-13. c, S7-37. See text for details and also ref. 18.

Generally, [Mn] and [U] on both sides of the crown are at detection limit, with [U] rising to a maximum of ~2 ppm for the final ~100 d of thin cervical enamel. Neither Sr/Ca nor Ba/Ca ratios are strongly affected by these minor [U] increases confirming the biogenic nature of the signal;

yet we note that some smaller Ba/Ca peaks co-occur with minor [U] peaks (for example, ~930 d; Fig. 3a). The consistency of the chronologies is attested by the high correspondence of the Sr/Ca signals between the two EDJ and prisms profiles. *Pongo* sp. SMF-8864 exhibits stark intratooth variability with three distinct peaks characterized by up to sixfold Sr/Ca and about eightfold Ba/Ca increases. This sixfold Sr/Ca change for the first peak (1.8×10^{-3} to 10.7×10^{-3}) decreases for the second and third peaks to threefold and twofold values, respectively. The influence of the Sr/Ca attenuation along prisms towards outer enamel²⁶ is discernible but partly compensated for in, for example, prism 3 by the strong biogenic signal (Fig. 3b). On the buccal side, three hypoplastic defects and four accentuated lines (AL) are present (Fig. 3c), yet these non-specific growth disturbances⁴⁷ are not coincident with the Sr/Ca (or Ba/Ca) trends. The interval between the midpoints of two consecutive peaks on the buccal aspect approximates 1 yr, namely 364 and 324 d between peaks 1 and 2 and peaks 2 and 3, respectively. The duration of these peaks is 95, 118 and 90 relative days for the first, second and third peaks, respectively, approximating an overall duration of 3 months each. The Sr/Ca profiles of the three *H. erectus* samples display low [U] and [Mn] and thus acceptable preservation, apart from localized peaks indicating spatially restricted diagenetic alteration (Fig. 4). Comparative elemental profiles for the lingual and buccal aspects of two *H. erectus* specimens presented in Extended Data Figs. 2 and 3 illustrate that enamel of the same tooth may be variably preserved yet we used the better-preserved domains. Limited intersample Sr/Ca variation ranges between 0.7 and 1.4×10^{-3} , while intraprofile Sr/Ca variability is 20–30%. These *H. erectus* Sr/Ca values are thus always below those in *Pongo* sp. SMF-8864, which is even more pronounced for the intrasample variability (20–30 versus 200–600%). The temporal spacing between broad Sr/Ca troughs and/or peaks in all samples lies between 340 and 380 d, consistent with approximately annual cyclicity. As it is uncertain which of the apparent minor Sr/Ca fluctuations are indicative of variable food intake or minor cryptic diagenetic overprint, we refrain from attributing unwarranted importance to small-scale variability. Despite the uncertain molar position for *H. erectus* SMF-8865, the stability of the Sr/Ca ratio in the first 220 d of tooth formation suggests the absence of the breastfeeding signal^{17,26}. Therefore, the tooth probably is not a first permanent molar, which starts to form earlier in life. We report sequentially microsampled stable carbon and oxygen isotope compositions of enamel derived from *H. erectus* S7-37 P4 ($n = 3$; Fig. 5 and Supplementary Table 1). The samples correspond to three distinct portions of the dental crown representing three partially overlapping life time moments. The $\delta^{13}\text{C}$ values range from -4.9‰ to -2.4‰ (average = $-3.9 \pm 1.4\text{‰}$ (1 s)), suggesting a diet which ranged from a dominated C4 plant consumption to a mixed C3/C4 plant consumption (54–72% C4 fraction in the diet, calculated after ref. 48). The $\delta^{18}\text{O}$ values remain stable with only very little variation between -6.7‰ and -5.9‰ (average = $-6.3 \pm 0.4\text{‰}$).

Discussion

Hominid Retzius periodicity RPs of 7–9 d for our sample of *H. erectus* teeth are typical of these Pleistocene hominins. They are similar to the periodicities reported previously for *H. erectus/ergaster* molars and premolars (7–8 and 9 d, respectively)²¹ but this apparent tighter distribution of values differs from the wider range of periodicities between 6 and 12 d characteristic of larger samples of living humans⁴⁹. An 8 d periodicity for the *Pongo* sp. lower molar SMF-8864 is slightly lower than the 9–12 d periodicity reported for fossil *Pongo* from Sumatra and mainland Asia⁵⁰ but lies within the range of values (8–11 d) reported for living *Pongo*⁵¹. Hominid trophic levels at Sangiran Trophic levels portray the relative position of species in a food web and are important for ecosystem functioning⁵². Fossil teeth of Carnivora

(Felidae), Perissodactyla (Rhinocerotidae) and Artiodactyla (Suidae, Cervidae and Hippopotamidae) from the Sangiran Dome with known trophic levels were used to establish an underlying relative trophic level framework for Sangiran. The ordering of fossil faunal taxa from Sangiran according to their enamel Sr/Ca ratios ($Sr/Ca_{\text{carnivores}} < Sr/Ca_{\text{omnivores}} < Sr/Ca_{\text{herbivores}}$) reflects trophic level differences that are in good agreement with their expected dietary habits (Fig. 2)11,53, suggesting reliable trophic level determination based on enamel Sr/Ca. The *Pongo* sp. lower molar SMF-8864 exhibits a high intratooth variability, caused by cyclical Sr/Ca peaks (Fig. 3) along the EDJ profile covering the whole range of other herbivorous specimens in this study. The average Sr/Ca ratios between the peaks is closer to the Sr/Ca ratio of herbivorous animals such as *Hexaprotodon* sp. and *Axis lydekkeri*54–57. The maximum Sr/Ca values for the first and second peaks are exceeding those of the rhinocerotids (for whom soil or dust ingestion might additionally lead to elevated Sr/Ca)32. The lowest Sr/Ca values in SMF-8864 overlap with those of suids and with the higher values of felids. This fits well with the known versatile diet of living orangutans, which includes fruits, flowers, bark, insects, eggs and occasionally meat58,59. The *H. erectus* lower molar SMF-8865 shows Sr/Ca ratios similar to *H. erectus* individuals S7-13 and S7-37. All *H. erectus* specimens in this study group with omnivorous (Suidae) and carnivorous (Felidae) mammals from Sangiran (Fig. 2), suggesting an omnivorous diet with a certain degree of meat consumption for *H. erectus* on Java. Comparison of Sr/Ca patterns in *H. erectus* and *Pongo* sp. The biogenic Sr/Ca peaks in *Pongo* sp. SMF-8864 occur nearly annually (Fig. 3). The Sr/Ca variation in *H. erectus* SMF-8865 also shows cyclical pattern: the duration of the cycle is ~345 d. *H. erectus* S7-13 shows a complete cycle of 347 d and a partial cycle of 148 d. The preserved portion of the crown ends before the end of the cycle. *H. erectus* S7-37 also shows two cycles with a duration of 375 and 383 relative days. The second cycle is marked by two smaller Sr/Ca decreases within the cycle. Uranium does not follow the annual cycle trend in any of the samples, thus suggesting negligible influence of diagenetic imprint (Fig. 4a–c). In summary, all *H. erectus* individuals demonstrate low-amplitude Sr/Ca cycles with a duration of ~1 yr, whereas *Pongo* sp. SMF-8864 demonstrates two cycles with sharp peaks that last 3–4 months. Diet of *Pongo* sp. reflects high seasonal food variability. The cyclical pattern of Sr/Ca and Ba/Ca peaks in *Pongo* sp. SMF-8864 with higher ratios occurring on an essentially annual basis gradually decreases within the ~3 yr of life represented by the tooth (Fig. 3). The repeatedly high Sr/Ca and Ba/Ca signals in this sample probably reflect annual periods with an increased intake of plant-based food resources, probably linked to a higher food availability during monsoonal periods, with a variation of the peak heights also linked to different food intake60. The duration and availability of food resources during the monsoon can fluctuate from season to season depending on monsoon intensity. This might be the reason for the oscillation of the amplitude of the Sr/Ca and Ba/Ca peaks. Studies of palaeosols and the occurrence of palaeoverisols in the Sangiran Dome strongly suggest that Java was a monsoon region in the Early Pleistocene, with an annual dry season3. Monsoonal rain forest was probably the preferred habitat of *Pongo* sp. on Java. Indeed, palaeoenvironmental reconstructions propose that Java was dominated by a mix of savannah, open woodlands and monsoonal rain forests during the Early to Middle Pleistocene3,61–63. Besides differences in food intake, the gradual decrease in Sr/Ca amplitude across the life time of the individual might also be influenced by the geometry of the tooth cusp to cervix, which might alter the expression of Sr and Ba relative to Ca. Increased maturation overprint, which is inversely proportional to enamel thickness, where Sr and Ba signals reduce towards the thinner cervical enamel of the tooth, was observed in a previous study26. One recent study suggested a causal relationship to a cyclical nursing pattern, resulting in a cyclical increase of Ba concentration in teeth (through the increased intake of

mothers' milk)⁶⁴. However, the synchronous up to sixfold increase in Sr/Ca and up to eightfold increase in Ba/Ca are unlikely to reflect a breastmilk signal because breastmilk is Sr-depleted through epithelial discrimination within the mammary glands^{17,26,65,66}. Recent studies on dentine and cementum in modern *Pongo* revealed that regions of [Sr] enrichment and depletion relate to both regular and irregular fluctuations in diet and Sr ingestion rather than to cyclical breastfeeding and may continue for as long as 20 yr into permanent canine tooth formation^{67,68}. Caloric intake in orangutans is two to three times greater during supra-annual masting events where several fruit and other plant food sources happen to ripen at the same time⁶⁰. Masting events are often then followed by periods of low fruit availability during dry periods, compensated in turn by orangutans burning fat reserves stored during mast-feeding⁶⁹. Sr/Ca and Ba/Ca signals might also be enhanced during episodes of mast-feeding because of geophagic behaviour, that is the deliberate ingestion of soils enriched in trace elements, which absorb toxins and tannins and which appear to alleviate gastrointestinal upsets⁶⁸. This behaviour was previously observed to be 'routine' in free-living orangutans⁷⁰. The sharp and relatively higher Sr/Ca and Ba/Ca signal of the first peak may perhaps represent an occasion where the supra-annual masting event coincided with the monsoon. It has been shown that non-specific stress enamel markers such as ALs can be correlated to variations in barium concentrations in dental tissues of primates⁷¹. In *Pongo* sp. SMF-8864 four ALs, occurring between the first and the second peaks (Fig. 3c), show a weak or absent correlation with elemental variations. However, the position of the ALs outside of the peaks' regions provide possible evidence of seasonal effects, as they might reflect stress events occurring during the first identified dry season. Hypoplastic defects on the tooth crown as a further sign of physiological stress do not correlate with elemental variations too (Fig. 3c) and indicate more complex, still-to-be-defined developmental deficiencies^{17,47}. Orangutans have the slowest life histories of any non-human primate with the latest weaning age of any mammal at around 7 yr but with relatively low levels of nutrient transfer during breastfeeding^{64,72–74}. Consequently, solid foods are supplemented in the infant's diet between 1 and 1.5 yr of age, to compensate additional nutritional demands^{64,73}. Infants can forage solid foods independently from the age of ~1.5 yr, whilst the mother is not decreasing her lactation efforts⁷³. Dry seasons with low food availability are compensated by extending weaning ages for infants leading to low growth and reproduction rates and solitary lifestyles^{69,75–77}. Dietary strategy of *H. erectus* The three *H. erectus* specimens show distinct Sr/Ca cycles with a duration of ~1 yr (Fig. 4). In contrast to the results from *Pongo* sp., the yearly Sr/Ca cycles in *H. erectus* are of low amplitude (20–30%), which are much smaller than the seasonal changes observed in *Pongo* sp. SMF- 8864. For *H. erectus*, these might reflect the consumption of specifically selected animal or plant resources, which were available in the regional context of a highly diverse ecosystem. Our $\delta^{13}\text{C}$ data show that the analysed *H. erectus* individual consumed a C4-dominated diet at the start of P4 mineralization and then changed to a consumption of a mix of C3 and C4 biomass in the later stages of tooth development (Fig. 5). *H. erectus* probably inhabited an open mosaic setting with the C3 signal indicating use of woodland/forest-edge habitats or gallery forests along rivers. The more C4-dominated diet suggests a tendency towards grasslands during the earlier period of tooth formation, possibly reflecting seasonal adaptations. The small variation of the relatively low $\delta^{18}\text{O}$ values (Fig. 5) of the analysed *H. erectus* indicates that the individual had access to a water source with only small fluctuations in $\delta^{18}\text{O}$ during the whole time of P4 tooth formation. Therefore, *H. erectus* possibly exploited regionally available resources and consumed water and/or aquatic foods from, for example, rivers. Nearly 70 km east of Sangiran, at the site of Trinil, where *H. erectus* was first discovered and described^{78,79}, it was suggested that members of this species probably consumed

aquatic resources like shellfish, indicating a high level of food resilience⁸⁰. In general, a high adaptive versatility is assumed for early members of the genus *Homo*⁸¹ and dental microwear traits in Sangiran *H. erectus* teeth also confirm an opportunistic omnivorous dietary strategy^{82,83}.

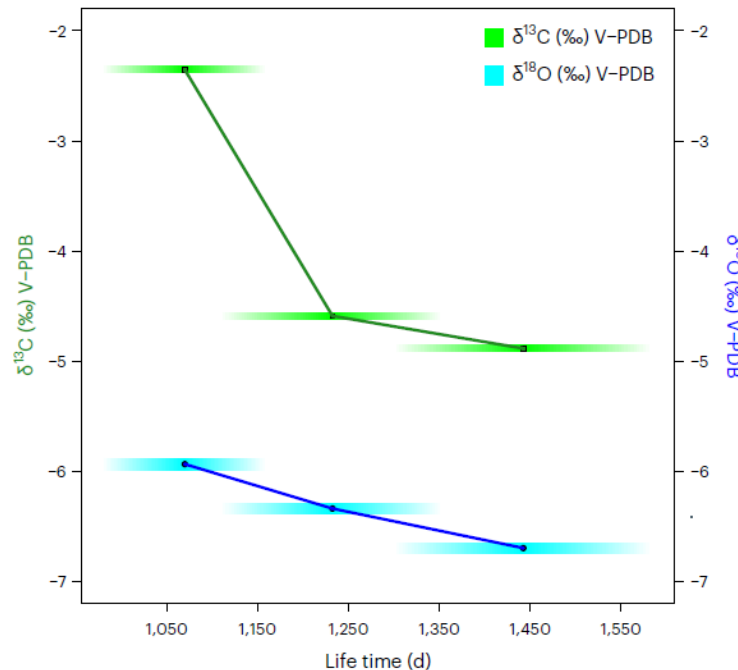


Fig. 5 | Carbon and oxygen isotope data of enamel from *H. erectus* S7-37 P4 plotted against life time in relative days and years. Length of coloured bars indicate possible formation times of enamel used for analyses and thickness indicates 1 s.d. of isotope data (0.03‰ for $\delta^{13}\text{C}$ and 0.05‰ for $\delta^{18}\text{O}$, respectively). V-PDB, Vienna Pee Dee Belemnite.

Conclusions The main outcome of the present study is the demonstration that both *Pongo* sp. and *H. erectus* at Sangiran had cyclical food resource availability with an annual periodicity. However, distinct differences in their chemical patterns point to dietary and life history differences of Pleistocene Southeast Asian *Pongo* sp. and *H. erectus*, both reacting to seasonal resource variations differently. While *Pongo* sp. consumed contrasting plant-based food resources during the wet (monsoonal) season presumably available in monsoonal rain forests, *H. erectus* was more versatile and exploited a broader range of high-diversity food resources along open mosaic habitats possibly with a tendency towards grasslands, as suggested by the carbon isotopic data. We demonstrate the effective use of histologically controlled time-resolved LA-ICPMS elemental analyses of hominid dental fossils to retrieve biogenic signals at subweekly time resolution. Our results show time-resolved geochemical analyses on *H. erectus* from the Sangiran Dome, which showcases the importance of geochemical analysis of fossil dental enamel of early humans to reconstruct past dietary behaviours and life histories in an evolutionary developmental perspective.

Methods Overall the methodologies used here follow those in refs. 17,26 and only a brief summary is given here below. Preparation, imaging and histological analysis of enamel thin sections^{84,85} were carried out at the Museo delle Civiltà in Rome. Sectioning was performed

using a Leica high-precision diamond blade (Leica AG) and IsoMet low-speed diamond blade microtome (Buehler). Sections were ground with Minimet 1000 Automatic Polishing Machine (Buehler) using silicon carbide grinding papers with two grits (1,000 and 2,500; Buehler). Sections were polished using a Minimet 1000 Automatic Polishing Machine (Buehler) with a microtissue damped with distilled water and diamond paste (Diamond DP-suspension M, Struers) containing 1 μm monocrystalline diamonds. Thickness of the faunal thin sections was 130–150 μm , depending on the preservation and visibility of the enamel microstructure. The hominid section thickness varied between 250 and 400 μm , thus facilitating the geochemical analysis but ensuring sufficient readability of the enamel microstructures. LA-ICPMS analyses LA-ICPMS analyses were carried out at the Frankfurt Isotope and Element Research Centre (FIERCE), Goethe University (Frankfurt). Histologically controlled tracks were determined on the enamel micrographs with Photoshop (Adobe). Sampling included continuous laser ablation tracks in enamel <100 μm parallel to the EDJ following the tooth growth direction²⁶. The LA-ICPMS system includes an 193 nm ArF excimer laser (RESOLUTION S-155; now Applied Spectra (ASI)) coupled to a two-volume laser ablation cell (Laurin Technic)^{26,86}. The laser ablation system is connected to an ICPMS Element XR (ThermoFisher Scientific) using nylon6 tubing. Thin sections were ultrasonically cleaned with methanol and fixed in the sample holder together with a series of primary and secondary standards. The micrographs with premarked laser tracks were uploaded in GeoStar μGIS Software (Norris Scientific) and retraced before LA analyses. LA-ICPMS data acquisition was performed in continuous path mode due to the benefits of a two-volume LA cell with fast signal washout and constant signal response^{26,86}. Before analysis, laser tracks were cleaned with a bigger spot size (40 μm), higher repetition rate (20 Hz) and scan speed (varying between 16.7 and 30 $\mu\text{m s}^{-1}$, depending on the size of teeth) to remove surface residues, which could alter the results⁸⁷. Analyses were carried out with a spot size of 18 μm , scan speed of 5 $\mu\text{m s}^{-1}$ and a repetition rate of 15 Hz. The time signal obtained from the ICPMS can be directly transferred to distance along the LA tracks via the constant scan speed of the laser X–Y stage; no time delays of the X–Y stage exist at waypoints of composite tracks²⁶. Between the LA system and the ICPMS, a signal smoothing device (squid) was included⁸⁶. The ICPMS (Element XR) detected the following isotopes from the ablated sample material (m/z): 25Mg, 27Al, 43Ca, 44Ca, 66Zn, 86Sr, 88Sr, 89Y, 138Ba, 140Ce, 208Pb and 238U. For calibration purposes (following ref. 88), NIST612 as a primary external standard and 44Ca as internal standard were used. In bioapatite, Ca is commonly used as an internal standard, which is set at 37% (refs. 26, 89, 90) but for elemental ratios no prior knowledge of the sample [Ca] is necessary. For NIST612 the following preferred values (± 2 s.d. (in %)) were used (from GeoREM website <http://georem.mpch-mainz.gwdg.de>): CaO, $11.9 \pm 0.4\%$ m/m; Zn, 38 ± 4 ; Sr, 78.4 ± 0.2 ; Y, 38 ± 2 ; Ba, 39.7 ± 0.4 ; Ce, 38.7 ± 0.4 ; Pb, 38.57 ± 0.2 ; and U, 37.38 ± 0.08 $\mu\text{g g}^{-1}$. Secondary standards with known concentrations and a matrix broadly similar to apatite (STDPx glasses) were analysed to assess accuracy and precision: STDP3-150, STDP3-1500, STDP5 (Ca-P-(Si) glass standards)⁹¹, KL2-G (basalt glass)⁹², MAPS5 (phosphate pellet) and MACS3 (Microanalytical Carbonate Standard; United States Geological Survey—preliminary Certificate of Analysis by S. Wilson), both available as ‘nano’ pellets from D. Garbe-Schönberg^{93,94}. MACS3 was used for Zn accuracy because no reported Zn values are available for the Ca-P-(Si) glass standard²⁶. Comparisons between measured secondary standard concentrations and reported concentrations revealed that the most accurate results with the lowest average bias were produced using the combination of NIST612 with 44Ca. Average relative biases of all three STDPx standards and MAPS5 were (in %): Al, -2.87 ± 3.26 ; Rb, 2.14 ± 20.47 ; Sr, 2.57 ± 4.98 ; Y, 5.85 ± 3.11 ; Ba, 0.68 ± 5.23 ; Ce, -1.31 ± 3.46 ; Pb, -2.88 ± 10.33 ; and U, 2.80

± 5.48 (average bias of all standards ± 1 s.d., in %). The compositional profiles displaying the concentration of elements relative to distance $d-1$ along the EDJ profile were smoothed with a locally weighted polynomial regression fit, with its associated standard error range (± 2 s.e.) for each predicted value⁹⁵. The software R (v.4.0.4) and the packages ‘lava’, ‘readxl’, ‘shape’ and ‘tidyverse’ were used for all statistical computations and generation of graphs. Elemental data were matched with odontochronologies of the *H. erectus* and *Pongo* sp. specimens by determining the chronology of each EDJ track after LA-ICPMS analysis (Extended Data Fig. 8) and directly assessing the enamel DSRs. DSR, in other words, the speed at which the ameloblast (the enamel forming cells) move towards the outer surface of the tooth is expressed in $\mu\text{m } d-1$ along the prisms^{96,97}, in the 100 μm region close to the EDJ. Carefully chosen histologically defined (EDJ) profiles facilitate the correlation between odontochronological and geochemical signals at a very high time resolution (<1 week). Isotopic ratio mass spectrometry analyses Stable carbon and oxygen analyses of S7-37 (right P4) were performed at the Goethe University-Senckenberg BiK-F Joint Stable Isotope Facility Frankfurt, Germany. For each sample, 2.9–3.8 mg of enamel powder was retrieved with a hand-held diamond tip dental drill. To produce sufficient sample material, drill holes were expended along to the growth axis of the enamel. To remove organic matter and potential diagenetic carbonate, enamel was pretreated with 2% NaOCl solution for 24 h followed by 1 M Ca-acetate acetic acid buffer solution for another 24 h and thoroughly rinsed with deionized water (modified after ref. ⁹⁸). Typically, enamel pretreatment resulted in $\sim 60\%$ mass loss. Then, 950–1,100 μg of pretreated enamel powder were reacted with 99% H_3PO_4 for 90 min at 70 °C in continuous flow mode using a Thermo Finnigan 253 mass spectrometer interfaced to a Thermo GasBench II. Analytical procedure followed the protocol of ref. ⁹⁹. Final isotopic ratios are reported versus V-PDB; overall analytical uncertainties are better than 0.3‰ for $\delta^{13}\text{C}$ and 0.05 for $\delta^{18}\text{O}$. Reporting summary Further information on research design is available in the Nature Portfolio Reporting Summary linked to this article.

Data availability

Data of elemental analyses and corresponding contextual information obtained in this study are available as Supplementary Data.

Acknowledgements

We express our gratitude to the Werner Reimers Foundation in Bad Homburg (Germany), which provides the Gustav Heinrich Ralph von Koenigswald collection as a permanent loan for scientific research to the Senckenberg Research Institute and Natural History Museum Frankfurt. FIERCE, where all LA-ICPMS analyses were performed, is financially supported by the Wilhelm and Else Heraeus Foundation and by the Deutsche Forschungsgemeinschaft (DFG, INST 161/921-1 FUGG and INST 161/923-1 FUGG), which are gratefully acknowledged. We thank L. Marko and A. Gerdes for help with analytical work. This is FIERCE contribution no. 113. We thank R. Brocke and G. Riedel for assistance with microscopic imaging. C.Z. acknowledges the support of the French CNRS (Centre National de la Recherche Scientifique). J.K. received funding from the Erasmus+ Traineeship programme (2019). A.N. received funding from the European Union’s Horizon 2020 research and innovation programme under the Marie Skłodowska-Curie grant agreement (no. 842812). T.L. received funding from the DFG (Emmy Noether Fellowship LU 2199/2-1).

Author contributions

The study was initiated by W.M., F.S. and J.K. and forms part of J.K.'s MSc research project completed under the supervision of W.M., L.B. and A.N. J.K., W.M., A.N., L.B., F.S. and O.K. designed research. J.K., W.M., A.N., L.B., B.P., T.L. and R.A. performed research. J.K., W.M., A.N., T.L., P.M. and L.B. analysed data. J.K., W.M., A.N., L.B., F.S., O.K., C.Z., T.L. and C.H. wrote the manuscript, with discussions on data interpretation and contributions to the manuscript text from M.C.D., N.B., A.-M.B. and F.D.

Competing interests

The authors declare no competing interests.

Additional information Extended data is available for this paper at <https://doi.org/10.1038/s41559-022-01947-0>.

Supplementary information

Supplementary material available at <https://doi.org/10.1038/s41559-022-01947-0>.

References

1. von Koenigswald, G. H. R. Fossil hominids from the Lower Pleistocene of Java. In *Report of the Eighteenth Session of the International Geological Congress* (ed. Butler, A. J.) 59–61 (International Geological Congress, 1948).
2. Grine, F. E. & Franzen, J. L. Fossil hominid teeth from the Sangiran Dome (Java, Indonesia). *Cour. Forsch. Inst. Senckenberg* 171, 75–103 (1994).
3. Bettis, E. A. et al. Way out of Africa: Early Pleistocene paleoenvironments inhabited by *Homo erectus* in Sangiran, Java. *J. Hum. Evol.* 56, 11–24 (2009).
4. Matsu'ura, S. et al. Age control of the first appearance datum for Javanese *Homo erectus* in the Sangiran area. *Science* 367, 210–214 (2020).
5. Weidenreich, F. Giant early man from Java and South China. *Anthropol. Pap. Am. Mus. Nat. Hist.* 40, 1–134 (1945).
6. von Koenigswald, G. H. R. *Pithecanthropus*, *Meganthropus* and the Australopithecinae. *Nature* 173, 795–797 (1954).
7. Franzen, J. L. in *Ancestors: The Hard Evidence* (ed. Delson, E.) 221–226 (Alan R. Liss, 1985).
8. Tyler, D. E. Sangiran 5, ('*Pithecanthropus dubius*'), *Homo erectus*, '*Meganthropus*,' or *Pongo*? *Hum. Evol.* 18, 229–241 (2003).
9. Tyler, D. E. An examination of the taxonomic status of the fragmentary mandible Sangiran 5, (*Pithecanthropus dubius*), *Homo erectus*, '*Meganthropus*,' or *Pongo*? *Quat. Int.* 117, 125–130 (2004).
10. Zanolli, C. et al. Evidence for increased hominid diversity in the Early to Middle Pleistocene of Indonesia. *Nat. Ecol. Evol.* 3, 755–764 (2019).
11. Balter, V., Braga, J., Télouk, P. & Thackeray, J. F. Evidence for dietary change but not landscape use in South African early hominins. *Nature* 489, 558–560 (2012).
12. Joannes-Boyau, R. et al. Elemental signatures of *Australopithecus africanus* teeth reveal seasonal dietary stress. *Nature* 572, 112–115 (2019).
13. Cerling, T. E. et al. Stable isotope-based diet reconstructions of Turkana Basin hominins. *Proc. Natl Acad. Sci. USA* 110, 10501–10506 (2013).
14. Lüdecke, T. et al. Dietary versatility of Early Pleistocene hominins. *Proc. Natl Acad. Sci. USA* 115, 13330–13335 (2018).

15. Wynn, J. G. et al. Isotopic evidence for the timing of the dietary shift toward C4 foods in eastern African *Paranthropus*. *Proc. Natl Acad. Sci. USA* 117, 21978–21984 (2020).
16. Smith, T. M. et al. Wintertime stress, nursing, and lead exposure in Neanderthal children. *Sci. Adv.* 4, 9483–9514 (2018).
17. Nava, A. et al. Early life of Neanderthals. *Proc. Natl Acad. Sci. USA* 117, 28719–28726 (2020).
18. Hoppe, K. A., Koch, P. L. & Furutani, T. T. Assessing the preservation of biogenic strontium in fossil bones and tooth enamel. *Int. J. Osteoarchaeol.* 13, 20–28 (2003).
19. Hinz, E. A. & Kohn, M. J. The effect of tissue structure and soil chemistry on trace element uptake in fossils. *Geochim. Cosmochim. Acta* 74, 3213–3231 (2010).
20. Bromage, T. G., Hogg, R. T., Lacruz, R. S. & Hou, C. Primate enamel evinces long period biological timing and regulation of life history. *J. Theor. Biol.* 305, 131–144 (2012).
21. Lacruz, R. S., Dean, M. C., Ramirez-Rozzi, F. & Bromage, T. G. Megadontia, striae periodicity and patterns of enamel secretion in Plio-Pleistocene fossil hominins. *J. Anat.* 213, 148–158 (2008).
22. Lacruz, R. S., Habelitz, S., Wright, J. T. & Paine, M. L. Dental enamel formation and implications for oral health and disease. *Physiol. Rev.* 97, 939–993 (2017).
23. Dean, M. C. Tooth microstructure tracks the pace of human life-history evolution. *Proc. R. Soc. B* 273, 2799–2808 (2006).
24. Smith, T. M. et al. Disentangling isolated dental remains of Asian Pleistocene hominins and pongines. *PLoS ONE* 13, e0204737 (2018).
25. Müller, W. & Anczkiewicz, R. Accuracy of laser-ablation (LA)-MC-ICPMS Sr isotope analysis of (bio)apatite—a problem reassessed. *J. Anal. Spectrom.* 31, 259–269 (2016).
26. Müller, W. et al. Enamel mineralization and compositional time-resolution in human teeth evaluated via histologically-defined LA-ICPMS profiles. *Geochim. Cosmochim. Acta* 255, 105–126 (2019).
27. Li, Q. et al. Spatially-resolved Ca isotopic and trace element variations in human deciduous teeth record diet and physiological change. *Environ. Archaeol.* 27, 474–483 (2022).
<https://doi.org/10.1080/14614103.2020.1758988>
28. Elias, R. W., Hirao, Y. & Patterson, C. C. The circumvention of the natural biopurification of calcium along nutrient pathways by atmospheric inputs of industrial lead. *Geochim. Cosmochim. Acta* 46, 2561–2580 (1982).
29. Burton, J. H., Price, T. D. & Middleton, W. D. Correlation of bone Ba/Ca and Sr/Ca due to biological purification of calcium. *J. Archaeol. Sci.* 26, 609–616 (1999).
30. Balter, V. et al. Ecological and physiological variability of Sr/Ca and Ba/Ca in mammals of West European mid-Würmian food webs. *Palaeogeogr. Palaeoclimatol. Palaeoecol.* 186, 127–143 (2002).
31. Pate, F. D. Bone chemistry and paleodiet. *J. Archaeol. Method Theory* 1, 161–209 (1994).
32. Kohn, M. J., Morris, J. & Olin, P. Trace element concentrations in teeth—a modern Idaho baseline with implications for archeometry, forensics, and palaeontology. *J. Archaeol. Sci.* 40, 1689–1699 (2013).
33. de Vos, J. in *Ancestors: The Hard Evidence* (ed. Delson, E.) 215–220 (Alan R. Liss, 1985).
34. de Vos, J. et al. The *Homo* bearing deposits of Java and its ecological context. *Cour. Forsch. Inst. Senckenberg* 171, 129–140 (1994).
35. Leinders, J. J. M. et al. The age of the hominid-bearing deposits of Java: state of the art. *Geol. Mijnb.* 64, 167–173 (1985).

36. Sondaar, P. Faunal evolution and the mammalian biostratigraphy of Java. *Cour. Forsch. Inst. Senckenberg* 69, 219–235 (1984).
37. Peek, S. & Clementz, M. T. Sr/Ca and Ba/Ca variations in environmental and biological sources: a survey of marine and terrestrial systems. *Geochim. Cosmochim. Acta* 95, 36–52 (2012).
38. Reynard, B. & Balter, V. Trace elements and their isotopes in bones and teeth: diet, environments, diagenesis, and dating of archeological and paleontological samples. *Palaeogeogr. Palaeoclimatol. Palaeoecol.* 416, 4–16 (2014).
39. Jacques, L. et al. Implications of diagenesis for the isotopic analysis of Upper Miocene large mammalian herbivore tooth enamel from Chad. *Palaeogeogr. Palaeoclimatol. Palaeoecol.* 266, 200–210 (2008).
40. Brumfitt, I. M., Chinsamy, A. & Compton, J. S. Depositional environment and bone diagenesis of the Mio/Pliocene Langebaanweg bonebed, South Africa. *S. Afr. J. Geol.* 116, 241–258 (2013).
41. Decrée, S. et al. The post-mortem history of a bone revealed by its trace element signature: the case of a fossil whale rostrum. *Chem. Geol.* 477, 137–150 (2018).
42. Janssen, R. et al. Tooth enamel stable isotopes of Holocene and Pleistocene fossil fauna reveal glacial and interglacial paleoenvironments of hominins in Indonesia. *Quat. Sci. Rev.* 144, 145–154 (2016).
43. Blumenthal, S. A. et al. Stable isotope time-series in mammalian teeth: in situ $\delta^{18}\text{O}$ from the innermost enamel layer. *Geochim. Cosmochim. Acta* 124, 223–236 (2014).
44. Zazzo, A., Balasse, M. & Patterson, W. P. High-resolution $\delta^{13}\text{C}$ intratooth profiles in bovine enamel: implications for mineralization pattern and isotopic attenuation. *Geochim. Cosmochim. Acta* 69, 3631–3642 (2005).
45. Deutsch, D. & Pe'er, E. Development of enamel in human fetal teeth. *J. Dent. Res.* 61, 1543–1551 (1982).
46. Dean, C. et al. Growth processes in teeth distinguish modern humans from *Homo erectus* and earlier hominins. *Nature* 414, 628–631 (2001).
47. Guatelli-Steinberg, D., Ferrell, R. J. & Spence, J. Linear enamel hypoplasia as an indicator of physiological stress in great apes: reviewing the evidence in light of enamel growth variation. *Am. J. Phys. Anthropol.* 148, 191–204 (2012).
48. Cerling, T. E. et al. Woody cover and hominin environments in the past 6 million years. *Nature* 476, 51–56 (2011).
49. Reid, D. J. & Dean, M. C. Variation in modern human enamel formation times. *J. Hum. Evol.* 50, 329–346 (2006).
50. Smith, T. M. Dental development in living and fossil orangutans. *J. Hum. Evol.* 94, 92–105 (2016).
51. Schwartz, G. T., Reid, D. J. & Dean, C. Developmental aspects of sexual dimorphism in hominoid canines. *Int. J. Primatol.* 22, 837–860 (2001).
52. Bonhommeau, S. et al. Eating up the world's food web and the human trophic level. *Proc. Natl Acad. Sci. USA* 110, 20617–20620 (2013).
53. Sponheimer, M. & Lee-Thorp, J. A. Enamel diagenesis at South African Australopith sites: implications for paleoecological reconstruction with trace elements. *Geochim. Cosmochim. Acta* 70, 1644–1654 (2006).
54. Eltringham, S. K. in *Pigs, Peccaries and Hippos* (ed. Oliver, W.) 55–60 (International Union for the Conservation of Nature and Natural Resources, 1993).

55. Jablonski, N. G. The hippo's tale: how the anatomy and physiology of Late Neogene Hexaprotodon shed light on Late Neogene environmental change. *Quat. Int.* 117, 119–123 (2004).
56. Hendier, A. *Diet Determination of Wild Pygmy Hippopotamus (Choeropsis liberiensis)*. MSc thesis, Univ. Neuchâtel (2019).
57. Klein, I. *Ernährung und ökologisches Profil von Axis lydekkeri*. MSc thesis, Goethe Univ. (2020).
58. Russon, A. E. et al. in *Orangutans: Geographic Variation in Behavioral Ecology and Conservation* (eds Wich, S. A. et al.) 135–156 (Oxford Univ. Press, 2009).
59. Kanamori, T. et al. Feeding ecology of Bornean orangutans (*Pongo pygmaeus morio*) in Danum Valley, Sabah, Malaysia: a 3-year record including two mast fruitings. *Am. J. Primatol.* 72, 820–840 (2010).
60. Kanamori, T., Kuze, N., Bernard, H., Malim, T. P. & Kohshima, S. Fluctuations of population density in Bornean orangutans (*Pongo pygmaeus morio*) related to fruit availability in the Danum Valley, Sabah, Malaysia: a 10-year record including two mast fruitings and three other peak fruitings. *Primates* 58, 225–235 (2017).
61. Sémah, A.-M., Sémah, F., Djubiantono, T. & Brasseur, B. Landscapes and hominids' environments: changes between the Lower and the early Middle Pleistocene in Java (Indonesia). *Quat. Int.* 4, 451 (2009).
62. Sémah, A. M. & Sémah, F. The rain forest in Java through the Quaternary and its relationships with humans (adaptation, exploitation and impact on the forest). *Quat. Int.* 249, 120–128 (2012).
63. Brasseur, B., Sémah, F., Sémah, A.-M. & Djubiantono, T. Approche paléopédologique de l'environnement des hominidés fossiles du dôme de Sangiran (Java central, Indonésie). *Quaternaire* 22, 13–34 (2011).
64. Smith, T. M., Austin, C., Hinde, K., Vogel, E. R. & Arora, M. Cyclical nursing patterns in wild orangutans. *Sci. Adv.* 3, e1601517 (2017).
65. Humphrey, L. T. Isotopic and trace element evidence of dietary transitions in early life. *Ann. Hum. Biol.* 41, 348–357 (2014).
66. Widdowson, E. M. Absorption, excretion and storage of trace elements: studies over 50 years. *Food Chem.* 43, 203–207 (1992).
67. Dean, C., Le Cabec, A., Spiers, K., Zhang, Y. & Garrevoet, J. Incremental distribution of strontium and zinc in great ape and fossil hominin cementum using synchrotron X-ray fluorescence mapping. *J. R. Soc. Interface* 15, 20170626 (2018).
68. Dean, M. C., Le Cabec, A., Van Malderen, S. J. M. & Garrevoet, J. Synchrotron X-ray fluorescence imaging of strontium incorporated into the enamel and dentine of wild-shot orangutan canine teeth. *Arch. Oral. Biol.* 119, 104879 (2020).
69. Pontzer, H., Raichlen, D. A., Shumaker, R. W., Ocobock, C. & Wich, S. A. Metabolic adaptation for low energy throughput in orangutans. *Proc. Natl Acad. Sci. USA* 107, 14048–14052 (2010).
70. Mahaney, W. C., Hancock, R. G. V., Aufreiter, S., Milner, M. W. & Voros, J. Bornean orangutan geophagy: analysis of ingested and control soils. *Environ. Geochem. Health* 38, 51–64 (2016).
71. Austin, C. et al. Uncovering system-specific stress signatures in primate teeth with multimodal imaging. *Sci. Rep.* 6, 18802 (2016).
72. Humphrey, L. T. Weaning behaviour in human evolution. *Semin. Cell Dev. Biol.* 21, 453–461 (2010).

73. van Noordwijk, M. A., Willems, E. P., Utami Atmoko, S. S., Kuzawa, C. W. & van Schaik, C. P. Multi-year lactation and its consequences in Bornean orangutans (*Pongo pygmaeus wurmbii*). *Behav. Ecol. Sociobiol.* 67, 805–814 (2013).
74. Galdikas, B. M. F. & Wood, J. W. Birth spacing patterns in humans and apes. *Am. J. Phys. Anthropol.* 83, 185–191 (1990).
75. van Noordwijk, M. A. & van Schaik, C. P. Development of ecological competence in Sumatran orangutans. *Am. J. Phys. Anthropol.* 127, 79–94 (2005).
76. Sugardjito, J., te Boekhorst, J. A. & van Hooff, J. A. R. A. M. Ecological constraints on the grouping of wild orangutans (*Pongo pygmaeus*) in the Gunung Leuser National Park, Sumatra, Indonesia. *Int. J. Primatol.* 8, 17–41 (1987).
77. Wich, S. A. et al. Life history of wild Sumatran orangutans (*Pongo abelii*). *J. Hum. Evol.* 47, 385–398 (2004).
78. Dubois, E. *Palaeontologische Onderzoekingen op Java* (Verslag van het Mijnwezen, 1891).
79. Dubois, E. *Pithecanthropus erectus, Einen Menschenaehnliche Uebergangsform aus Java* (G.E. Stechert (Alfred Hafner), 1894).
80. Joordens, J. C. A. et al. *Homo erectus* at Trinil on Java used shells for tool production and engraving. *Nature* 518, 228–231 (2015).
81. Ungar, P. S., Grine, F. E. & Teaford, M. F. Diet in early *Homo*: a review of the evidence and a new model of adaptive versatility. *Annu. Rev. Anthropol.* 35, 209–228 (2006).
82. Tausch, J. *A New Method for Examining Hominin Dietary Strategy: Occlusal Microwear Vector Analysis of the Sangiran 7 Homo erectus Molars* (Goethe Univ., 2011).
83. Tausch, J., Kullmer, O. & Bromage, T. G. A new method for determining the 3D spatial orientation of molar microwear. *Scanning* 37, 446–457 (2015).
84. Caropreso, S. et al. Thin sections for hard tissue histology: a new procedure. *J. Microsc.* 199, 244–247 (2000).
85. Bondioli, L., Nava, A., Rossi, P. F. & Sperduti, A. Diet and health in central-southern Italy during the Roman Imperial time. *Acta IMEKO* 5, 19–25 (2016).
86. Müller, W., Shelley, M., Miller, P. & Broude, S. Initial performance metrics of a new custom-designed ArF excimer LA-ICPMS system coupled to a two-volume laser-ablation cell. *J. Anal. At. Spectrom.* 24, 209–214 (2009).
87. Evans, D. & Müller, W. LA-ICPMS elemental imaging of complex discontinuous carbonates: an example using large benthic foraminifera. *J. Anal. At. Spectrom.* 28, 1039–1044 (2013).
88. Longerich, H. P., Jackson, S. E. & Günther, D. Laser ablation inductively coupled plasma mass spectrometric transient signal data acquisition and analyte concentration calculation. *J. Anal. At. Spectrom.* 11, 899–904 (1996).
89. Retief, D. H., Cleaton-Jones, P. E., Turkstra, J. & De Wet, W. J. The quantitative analysis of sixteen elements in normal human enamel and dentine by neutron activation analysis and high-resolution gamma-spectrometry. *Arch. Oral. Biol.* 16, 1257–1267 (1971).
90. Lacruz, R. S. Enamel: molecular identity of its transepithelial ion transport system. *Cell Calcium* 65, 1–7 (2017).
91. Klemme, S. et al. Synthesis and preliminary characterisation of new silicate, phosphate and titanite reference glasses. *Geostand. Geoanal. Res.* 32, 39–54 (2008).
92. Jochum, K. P. et al. Accurate trace element analysis of speleothems and biogenic calcium carbonates by LA-ICP-MS. *Chem. Geol.* 318–319, 31–44 (2012).
93. Garbe-Schönberg, D. & Müller, S. Nano-particulate pressed powder tablets for LA-ICP-MS. *J. Anal. At. Spectrom.* 29, 990–1000 (2014).

94. Jochum, K. P. et al. Nano-powdered calcium carbonate reference materials: significant progress for microanalysis? *Geostand. Geoanal. Res.* 43, 595–609 (2019).
95. Cleveland, W. S., Grosse, E. & Shyu, W. M. in *Statistical Models in S* (eds Chambers, J. M. & Hastie, T.) 309–376 (Chapman and Hall/ CRC, 1992).
96. Guatelli-Steinberg, D., Floyd, B. A., Dean, M. C. & Reid, D. J. Enamel extension rate patterns in modern human teeth: two approaches designed to establish an integrated comparative context for fossil primates. *J. Hum. Evol.* 63, 475–486 (2012).
97. Birch, W. & Dean, M. C. A method of calculating human deciduous crown formation times and of estimating the chronological ages of stressful events occurring during deciduous enamel formation. *J. Forensic Leg. Med.* 22, 127–144 (2014).
98. Koch, P. L., Tuross, N. & Fogel, M. L. The effects of sample treatment and diagenesis on the isotopic integrity of carbonate in biogenic hydroxylapatite. *J. Archaeol. Sci.* 24, 417–429 (1997).
99. Spötl, C. & Vennemann, T. W. Continuous-flow isotope ratio mass spectrometric analysis of carbonate minerals. *Rapid Commun. Mass Spectrom.* 17, 1004–1006 (2003).